ELSEVIER

Polymer 40 (1999) 6417–6428

polymer

All sol–gel organic–inorganic nonlinear optical materials based on melamines and an alkoxysilane dye

G.-H. Hsiue[a,*], R.-H. Lee[a], R.-J. Jeng[b]

[a]*Department of Chemical Engineering, National Tsing Hua University, Hsinchu 30043, Taiwan*
[b]*Department of Chemical Engineering, National Chung Hsing University, Taichung, Taiwan*

Received 8 April 1998; received in revised form 18 August 1998; accepted 28 December 1998

Abstract

A series of all sol–gel organic–inorganic nonlinear optical materials based on the prepolymers of melamines and an alkoxysilane dye (ASD) were investigated. The NLO-active ASD containing nitroazobenzene was incorporated into the melamine matrices with different weight ratios. This all sol–gel type is shown to have the advantages of simultaneous polymerizations, and better compatibility between two components due to residual hydroxyl and silanol groups after curing. The simultaneous route is often used to avoid significant phase separation in a multi-component system. SEM results indicate that the inorganic networks are distributed uniformly throughout the organic networks on a molecular scale. The silica particle sizes are well under 1 μm. This series of all sol–gel materials exhibits large second-order optical nonlinearity ($d_{33} = 10–54$ pm/V at 1064 nm, and 3–17 pm/V at 1542 nm) after poling and curing. Temporal stability of the effective second harmonic coefficient at 100°C is also reported.

Keywords: Sol–gel; Melamines; Alkoxysilane dye

1. Introduction

Second-order nonlinear optical (NLO) polymers have been extensively studied for applications in photonic devices, such as frequency doubling and electro-optical (EO) modulation, because of their large optical nonlinearity, excellent processibility, low dielectric constants, and high laser damage thresholds [1]. Over the past few years, different approaches have been investigated for preparing NLO polymers with excellent NLO properties. They are guest–host system, side-chain type, main-chain type, and crosslinked type NLO polymers [2–8]. One of the crosslinked NLO polymers is the sol–gel material [6–8]. Sol–gel materials with second-order NLO properties are promising for applications in photonic devices for a number of reasons. These include their low temperature processing capability, excellent optical quality, good thermal and temporal stabilities, refractive index control of films, and ease of device fabrication [6–8]. A sol–gel matrix doped with NLO chromophores has been reported by Jeng et al. [6]. Moreover, NLO-active dyes have been covalently bonded with alkoxysilanes [7,8]. Subsequently, organically modified inorganic NLO sol–gel materials were obtained.

Recently, organic–inorganic sol–gel materials have received significant attention, especially for advanced photonics applications [9–11]. By incorporating the hardness of an inorganic sol–gel material into a high performance organic polymer, the resulting organic–inorganic composite may display the desired properties of both components [12–14]. The incorporation of an inorganic sol–gel material provides an inert environment for the organic polymer and theoretically prevent its thermal decomposition. Moreover, the inorganic networks will be densely and uniformly packed throughout the organic chain segments by the sol–gel process [12–14]. The interactions between an inorganic oxide and an organic polymer will reduce the molecular motions during the glass transition [14]. Therefore, the incorporation of an inorganic NLO sol–gel material within an organic polymer is a reasonable approach to enhance long-term NLO stability.

Melamine-based sol–gel materials have been widely used in the lighting, coating, and decorating industries because of their good transparency [15]. High crosslink density with uniformity can be obtained via a sol–gel process involving sequential hydrolysis and condensation reactions [16,17]. Based on these conclusions, melamine is chosen to be the organic component of an all sol–gel organic–inorganic NLO material. There are other reasons for choosing this all sol–gel type organic–inorganic material. Water

* Corresponding author. Tel.: + 886-35-719-956; fax: + 886-35-726-525.

0032-3861/99/$ - see front matter
PII: S0032-3861(99)00024-5

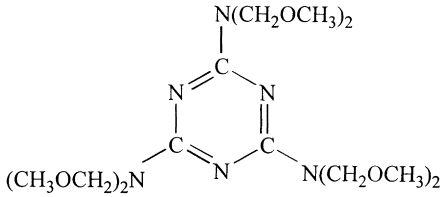

(a) HMM1

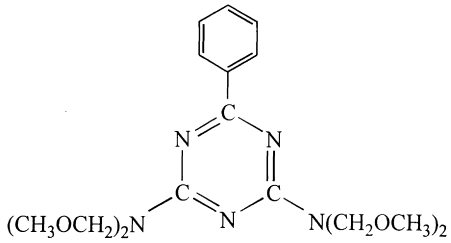

(b) HMM2

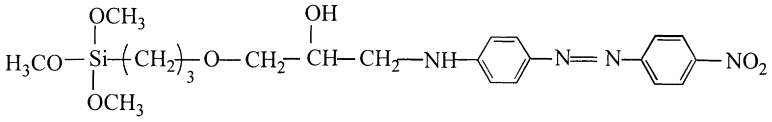

(c) ASD

Fig. 1. Chemical structures of: (a) HMM1; (b) HMM2; and (c) ASD.

produced from simultaneous sol–gel reactions aids subsequent hydrolysis of the melamine and alkoxysilane. Moreover, this simultaneous route is often used to avoid phase separation of a multicomponent system [18–20]. One more important feature of this all sol–gel type is that the residual hydroxyl groups and silanol groups after curing will be shown to exhibit hydrogen-bonding interactions between silicon oxide and organic networks. This would promote the compatibility between the inorganic and organic network. For the sake of comparison, a novel organically modified sol–gel system was developed by the sol–gel processing of the ASD and a melamine end-capped with alkoxysilane.

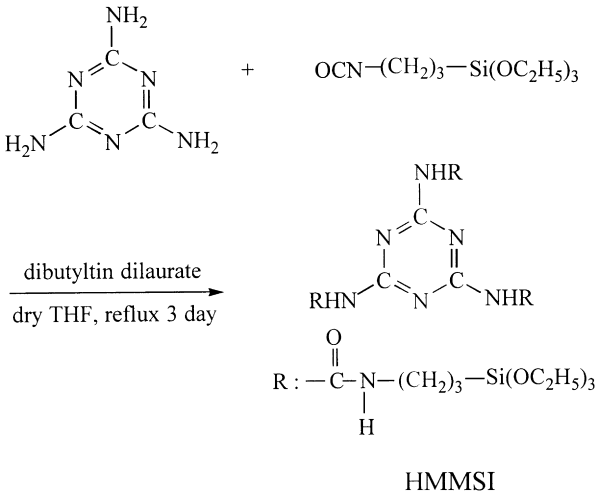

Scheme 1. Synthesis of the triethoxysilane capped melamine HMMSI.

The thermal behavior of these all sol–gel NLO materials was studied by their temperature dependence on dielectric relaxation. The phase homogeneity was analyzed using scanning electron microscopy (SEM). Further, the second-order nonlinearity and temporal stability at 100°C were also investigated.

2. Experimental

Hexa(methoxymethyl)melamine, HMM1 (Fig. 1(a)) and (hydroxymethyl)benzoquanamine, HMM2 (Fig. 1(b)) were obtained from Monsanto and Aldrich, respectively, and were used as received. The prepolymers of HMM1 and HMM2 were prepared by heating the monomer at 220°C for 1 h in the presence of acetic acid. The alkoxysilane dye, ASD (Fig. 1(c)) was synthesized by the coupling of a monoepoxy of (3-glycidoxypropyl) trimethoxysilane and a monoamine of 4-[(4′-nitrophenyl)azo]phenylamine

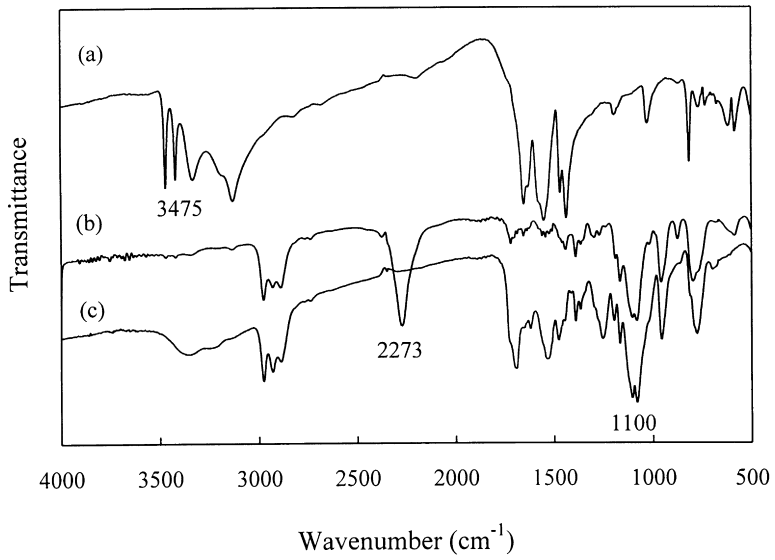

Fig. 2. Infrared spectra of: (a) melamine; (b) 3-isocyanatopropyl triethoxysilane; and (c) HMMSI.

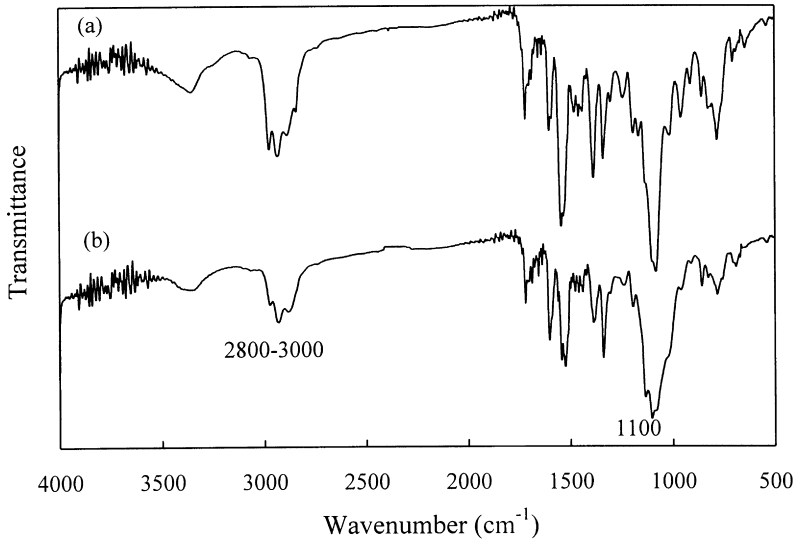

Fig. 3. Infrared spectra of M2ASD50 (HMM2 : ASD = 1 : 1), from top to bottom: pristine, cured (220°C, 1 h).

Table 1
Thermal behavior of a series of melamine (HMM1, HMM2, and HMMSI) and an alkoxysilane dye (ASD) based all sol–gel NLO materials

Samples[a]	Composition (weight ratio)	T_d (°C)[b]
ASD	—	293.0
M1ASD75	HMM1/ASD (25/75)	284.5
M1ASD50	HMM1/ASD (50/50)	268.0
M1ASD25	HMM1/ASD (75/25)	263.6
M2ASD75	HMM2/ASD (25/75)	291.2
M2ASD50	HMM2/ASD (50/50)	275.3
M2ASD25	HMM2/ASD (75/25)	267.4
MSIASD75	HMMSI/ASD (25/75)	288.7
MSIASD50	HMMSI/ASD (50/50)	277.1
MSIASD25	HMMSI/ASD (75/25)	269.6

[a] Samples were cured at 220°C for 1 h.
[b] T_d was calculated at the temperature corresponding to 5% weight loss.

(Disperse Orange 3) [21]. Moreover, the preparation of triethoxysilane capped melamine (HMMSI) was achieved by the functional reaction of 3-isocyanatopropyl triethoxysilane and melamine (Scheme 1). Melamine, 2.5 g, (0.02 mol) was added to the dry tetrahydrofuran (THF) (80 ml) and the mixture was refluxed while being stirred under nitrogen and catalyst (dibutyltin dilaurate) for 1 h. Then, 3-isocyanatopropyl triethoxysilane, 12 g, (0.06 mol) was added and the heating was continued for 3 days. The functional reaction was monitored during the reaction by FTIR spectroscopy. The product was further extracted with ethyl acetate. After the solvent was removed, the residue was purified by column chromatography. The final clear and almost colorless viscous product was obtained. The chemical structure of HMMSI was characterized using FTIR spectroscopy. The infrared spectra of melamine,

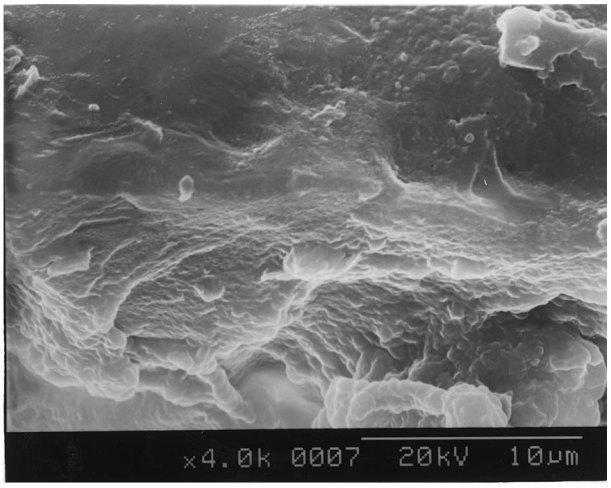

(a)

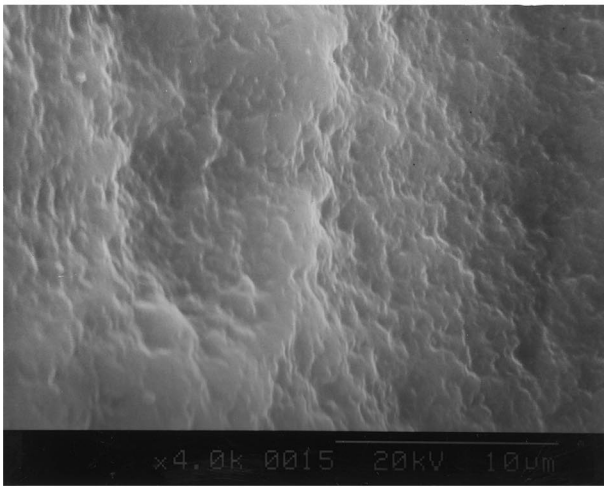

(b)

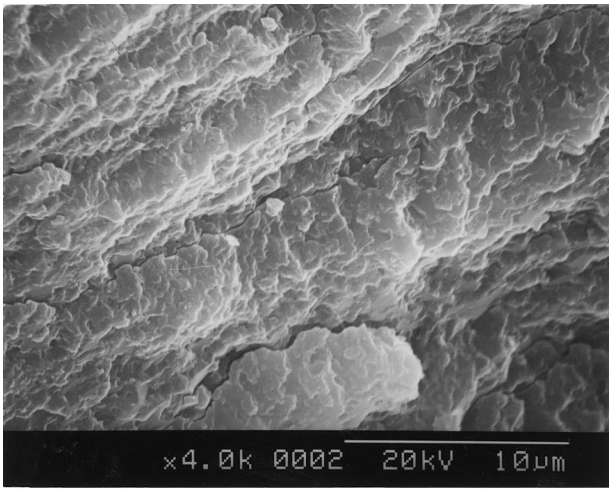

(c)

Fig. 4. Scanning electron micrograph of the cured: (a) M1ASD50; (b) M2ASD50; and (c) MSIASD50.

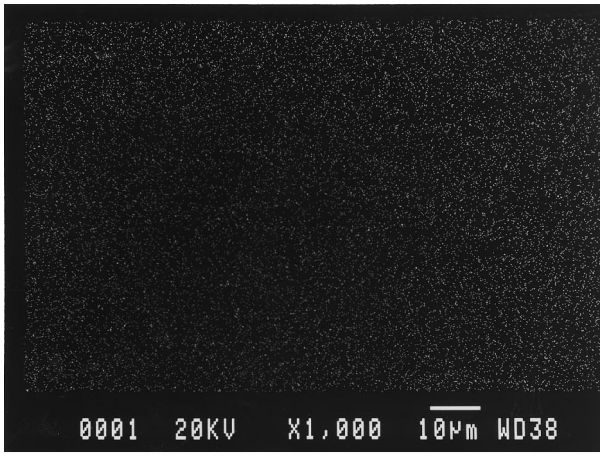

(a)

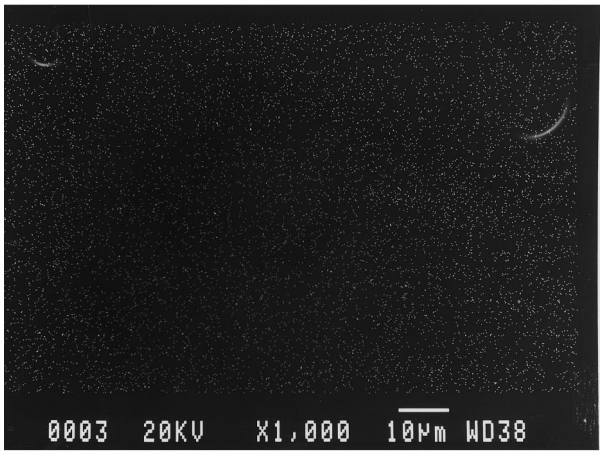

(b)

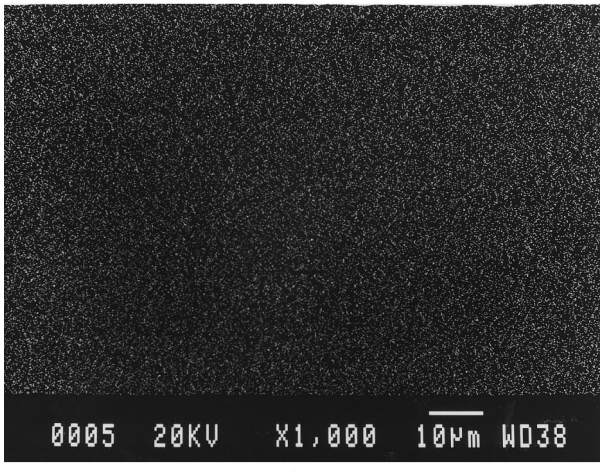

(c)

Fig. 5. The mapping spectra of the cured: (a) M1ASD50; (b) M2ASD50; and (c) MSIASD50.

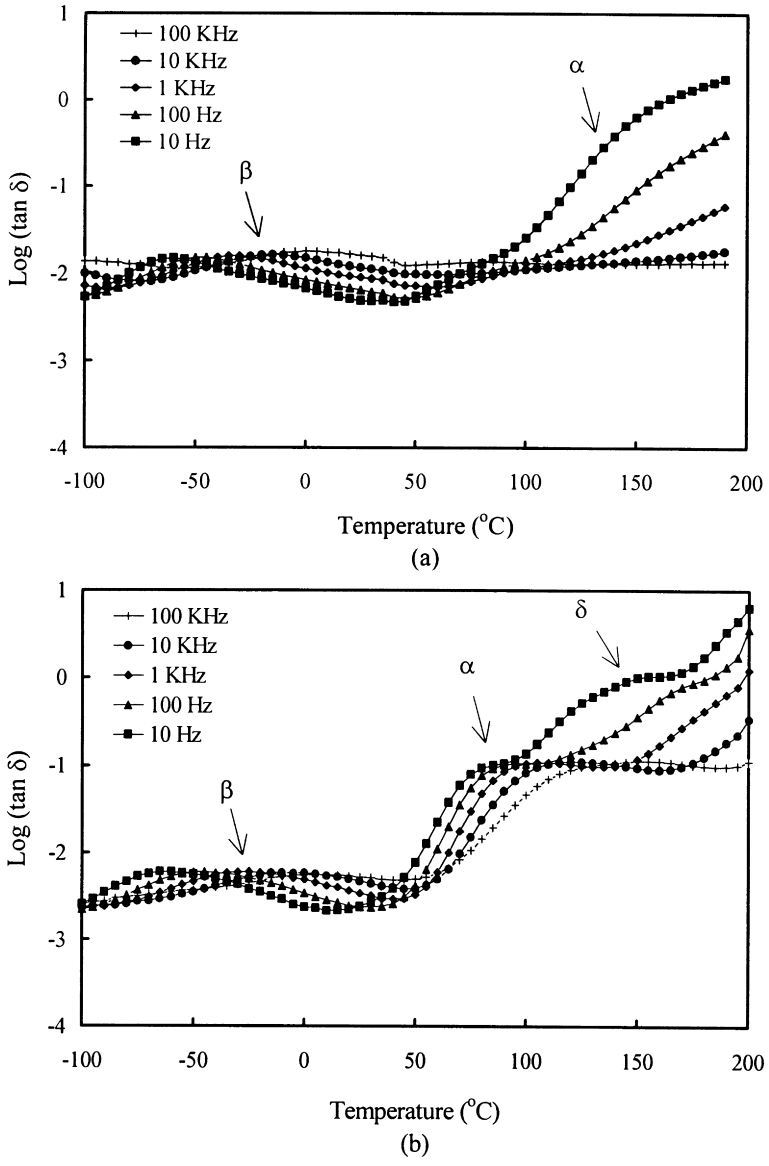

Fig. 6. Dielectric loss tangent versus temperature and frequency for the cured: (a) HMM1; and (b) ASD.

3-isocyanatopropyl triethoxysilane, and HMMSI are shown in Fig. 2. The NH_2 stretch of melamine was observed around 3500 cm^{-1}. For 3-isocyanatopropyl triethoxysilane, the C–H vibration stretch of O–R showed up at around 2800–3000 cm^{-1}. The Si–O–C stretching frequencies of alkoxysilane are located in the region of 1000–1100 cm^{-1}. The strong absorption peak corresponding to N=C=O stretching was observed at 2273 cm^{-1}. For HMMSI sample, the stretching peak of N=C=O group disappeared at 2273 cm^{-1}. This indicates that the residual 3-isocyanatopropyl triethoxysilane was completely removed by column chromatography. In addition, the NH_2 stretch of melamine was not observed around 3500 cm^{-1}. The C–H vibration stretch of O–R and Si–O–C stretch of alkoxysilane were observed at around 2800–3000 and 1000–1100 cm^{-1}, respectively. These results indicate that the HMMSI was obtained.

The reaction behavior of the materials was determined by differential scanning calorimetry, DSC, (Seiko SSC/5200) at a heating rate of 10°C min^{-1}. Degradation temperatures (T_d) were measured on a Seiko Exstar 6000 thermogravimetric analyzer (TGA) at 10°C min^{-1} under air. UV-Vis spectra were recorded on a Perkin Elmer Lambda 2S spectrophotometer. The crosslinking of these sol–gel materials was characterized by Fourier transform infrared (FTIR) spectroscopy (Bio-Rad FTS155 FTIR). SEM (Jeol JEM-840A) was used to study the morphology of the film (gold coated). Dielectric relaxation behavior of the NLO sol–gel materials was studied by dielectric spectroscopy, DEA, (Novercontrol GmbH). The measurement was performed

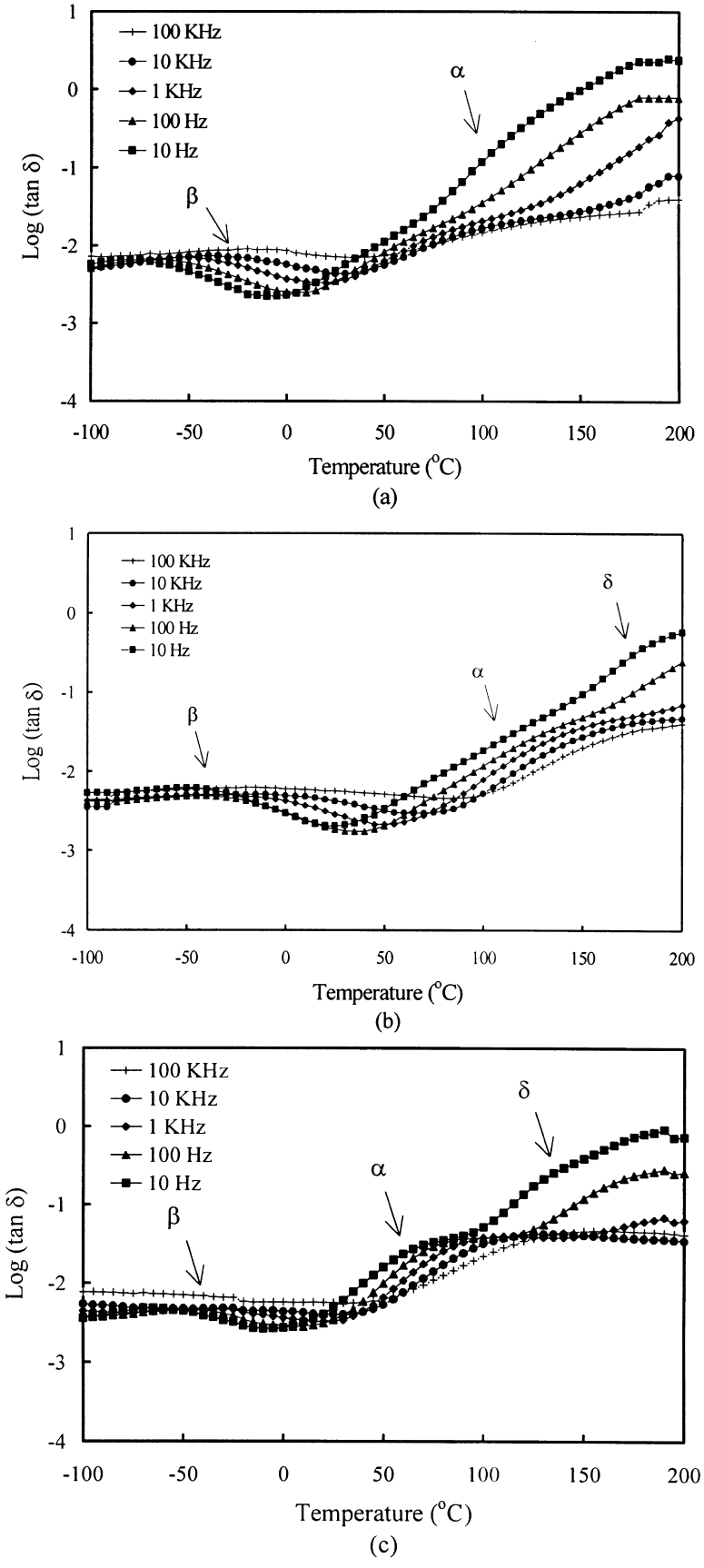

Fig. 7. Dielectric loss tangent versus temperature and frequency for the cured: (a) M1ASD25; (b) M1ASD50; and (c) M1ASD75.

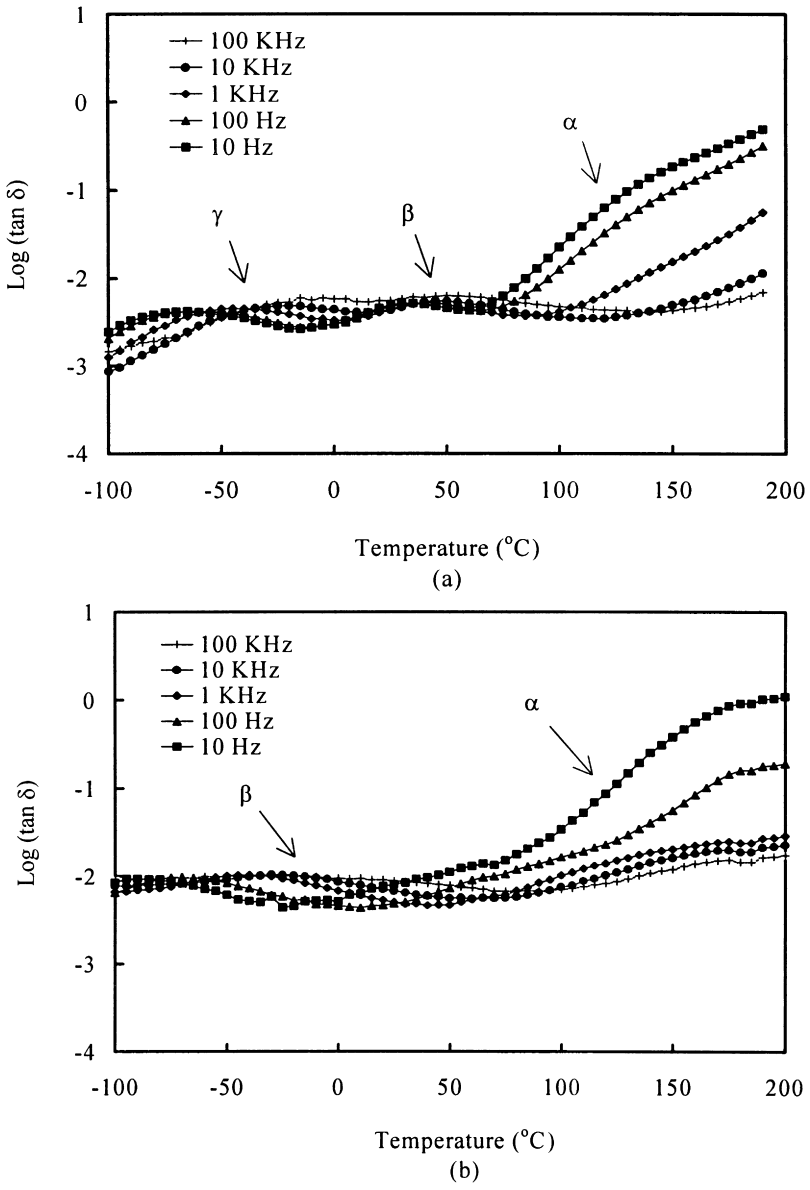

Fig. 8. Dielectric loss tangent versus temperature and frequency for the cured: (a) HMM2; and (b) M2ASD50.

using a Schlumberger SI 1260 impedance/gain-phase analyzer and a Quator temperature controller. Dielectric measurements were made from −100°C to 250°C. The frequency scan range was from 10^{-1} to 10^{6} Hz.

A prepolymer solution containing the ASD and melamine-based prepolymer was prepared for spin-coating. In one example, the ASD (0.1 g) and prepolymer (0.1 g) (weight ratio = 1 : 1) were dissolved in THF (0.1 g), containing 20 mg of water and 20 mg of acetic acid to aid the hydrolysis of ASD and the melamine-based prepolymer. The prepolymer solution was stirred at room temperature for 4 h. Thin films were prepared by spin-coating the polymer solution onto indium tin oxide (ITO) glass substrates. The poling process for the second-order NLO polymer films was carried out using an in-situ poling technique. The details of the corona poling set-up were the same as previously reported [22]. The poling process was started at room temperature and increased to 220°C at a heating rate of 15°C min^{-1}. The corona current was maintained at 2 μA with a potential of 4.5 kV, while the poling temperature was kept at 220°C for 1 h. The formation of the network and the molecular alignment of the poled order proceeded simultaneously during this period. Upon saturation of the SHG signal intensity, the sample was then cooled down to room temperature in the presence of the poling field, at which point the poling field was terminated. The thickness and indices of refraction for the NLO polymer films were measured by a prism coupling (Metricon 2010). Second harmonic generation measurements were carried out with a Q-switched Nd–YAG laser operating at 1064 and

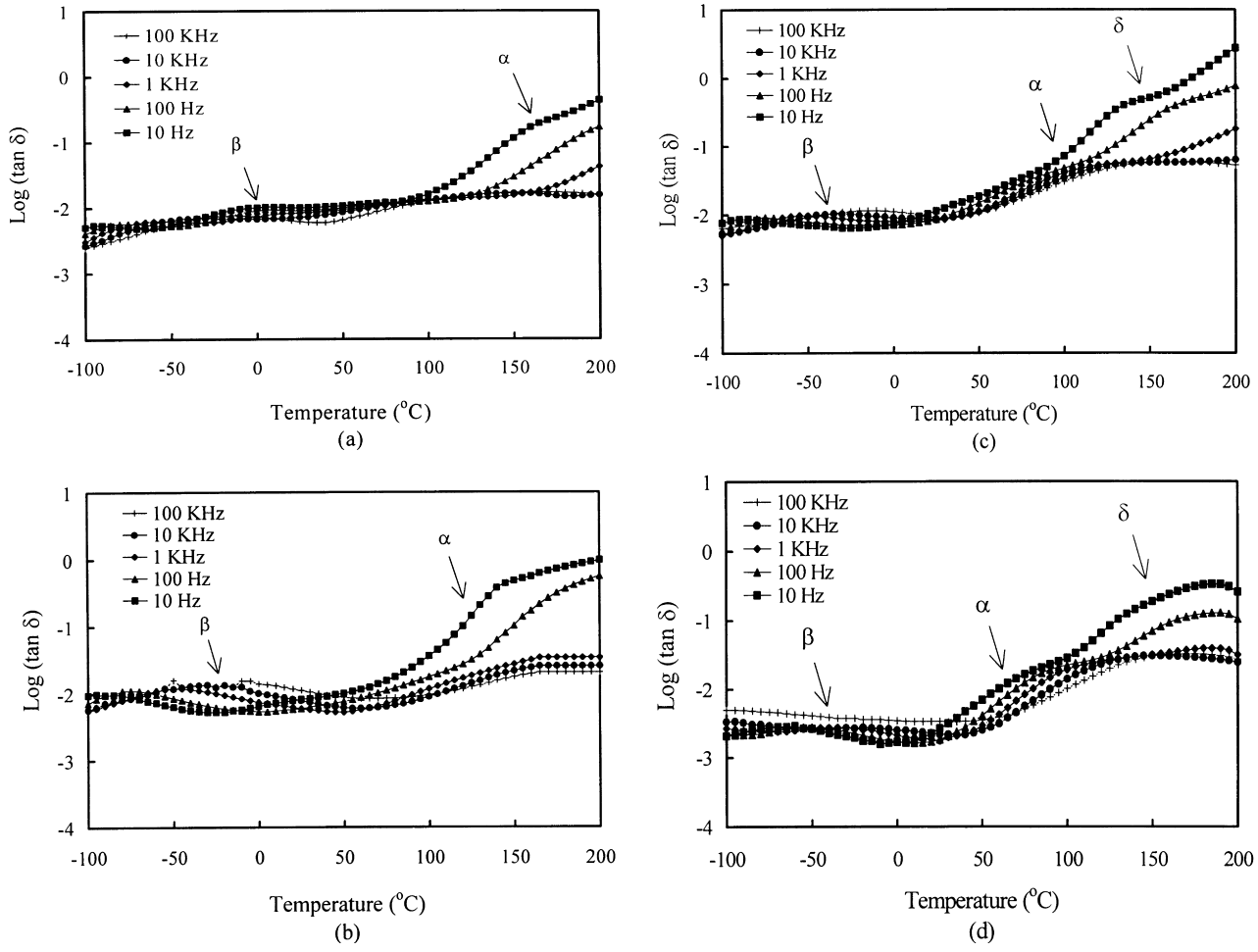

Fig. 9. Dielectric loss tangent versus temperature and frequency for the cured: (a) HMMSI; (b) MSIASD25; (c) MSIASD50; and (d) MSIASD75.

1542 nm using a Raman cell [23]. Measurement of the second harmonic coefficient, d_{33}, has been previously discussed [24], and the d_{33} values were corrected for absorption [25].

3. Results and discussion

In this study, the optimum curing conditions were determined using the DSC reaction scan for sol–gel process. The curing temperature (220°C) was chosen as the approximate midpoint between the start of exothermic curing and the thermal decomposition temperature of ASD [26]. In addition, the thermal fluctuation at a high poling temperature would negatively affect the non-centrosymmetric alignment of the NLO chromophores. This was also taken into consideration in determining the optimum curing parameters. After curing the organic–inorganic sample M2ASD50 (HMM2:ASD = 50:50), the formation of the Si–O–Si was evidenced by FTIR spectroscopy (Fig. 3). An appreciable decrease of the C–H vibrational stretch of the O–CH_3 groups at around 2800–3000 cm^{-1} was observed which is due to the condensation of the methoxymethyl groups. Moreover, the absorption peak at around 1100 cm^{-1} is broader after curing, suggesting Si–O–Si formation [26]. In addition, thermal decomposition of the sol–gel materials was measured on a thermogravimetric analyzer under air after curing at 220°C for 1 h. T_d was read at the temperature corresponding to a weight loss of 5%. The composition and the T_d of the all sol–gel organic–inorganic NLO materials are summarized in Table 1. The T_d of the organic–inorganic NLO sol–gel materials increase with the increase in the content of ASD because of a higher inorganic ratio.

Thin films were prepared by spin-coating the prepolymer solution onto ITO glass substrates for NLO measurement. Optical clarity was maintained before and after the poling and curing process for these all sol–gel organic–inorganic NLO materials. This was confirmed using optical microscopy. Moreover, the homogeneity of these organic–inorganic sol–gel materials was studied using SEM. The fractured surfaces of the cured M1ASD50, M2ASD50 and MSIASD50 are shown in Fig. 4. No sign of any phase separation was observed when the magnification was increased up to 4000×. In addition, the distribution of inorganic networks in the organic matrix was further confirmed using SEM with a mapping technique [27]. The mapping

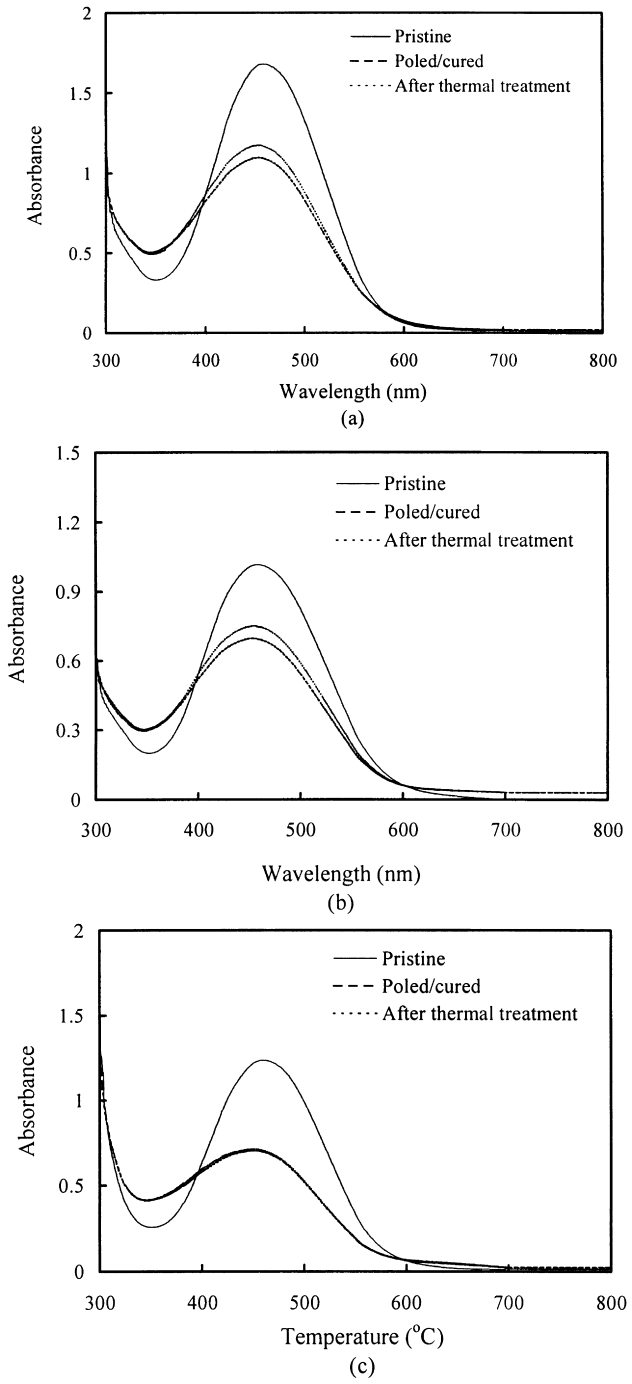

Fig. 10. UV-Vis absorption spectra of the: (a) M1ASD50; (b) M2ASD50; and (c) MSIASD50.

spectra of the cured M1ASD50, M2ASD50 and MSIASD50 are shown in Fig. 5. The results indicate that the silicons are distributed uniformly throughout the polymer film and that the silica particle sizes are much smaller than 1 μm for these samples [27]. The observation by SEM supports the fact that a high degree of uniform mixing between the organic and inorganic networks was obtained for these melamine-based sol–gel composites.

Glass transition temperatures (T_g) were not detectable from the DSC study for the cured organic–inorganic sol–gel NLO materials because of the formation of high crosslinking density of the organic and inorganic networks [28]. Dielectric relaxation is a useful technique for studying the dynamic behavior of the polymers, as it is sensitive to the motions of the ground-state dipole moments of the NLO chromophores. Moreover, the molecular mobility is determined by the molecular packing of the organic and inorganic networks. The packing structure of the organic–inorganic sol–gel material could be thoroughly examined by the dielectric relaxation behavior. Temperature dependence of the dielectric loss tangent for the cured HMM1 and ASD is shown in Fig. 6. For cured HMM1, the β-relaxation was observed from −100°C to 50°C, which corresponded to the local (i.e. crankshaft) motion of the methylene or methylene–ether bridges in the network and the free motion of the dangling chains from the unreacted methoxymethyl groups (Fig. 6(a)) [29]. Moreover, the α-relaxation (associated with the glass transition) occurred at a higher temperature range. The large amplitude of the α-relaxation implies a low crosslinking density of the cured HMM1 [12]. In Fig. 6(b), the β-relaxation was observed in the range of −100°C–50°C, which corresponds to the local and non-cooperative motions of the NLO chromophore for cured ASD. Moreover, the α and δ-relaxations occurred at a higher temperature range. The δ-relaxation was associated with a larger scale of molecular motion, which has a lower relaxation frequency (below 1 kHz) than the α-relaxation (10 Hz–100 kHz) [30]. The amplitude of the α-relaxation is significant, which also reflects that the cured ASD has a low crosslink density. For the cured M1ASD25, M1ASD50 and M1ASD75 (Fig. 7), the suppressed α-relaxation peaks were located at higher temperatures as compared to the cured ASD. In particular, the M1ASD50 sample exhibited a highest α-relaxation temperature. In Fig. 7(a), the relaxation behavior of the cured M1ASD25 was similar to that of the cured HMM1 because of the high content of HMM1. Moreover, relaxation behavior of the cured M1ASD75 with high ASD content was similar to the cured ASD (Fig. 7(c)).

Table 2
Linear optical properties of a series of melamines and an alkoxysilane dye based all sol–gel NLO materials. (d is the thickness of the polymer film. n_{532}, n_{771}, n_{1064}, n_{1542} are the refraction indices at 532, 771, 1064, and 1542 nm, respectively.)

Samples	d (μm)	n_{532}	n_{771}	n_{1064}	n_{1542}
ASD	1.1	1.75	1.67	1.64	1.61
M1ASD75	1.0	1.71	1.65	1.63	1.59
M1ASD50	0.9	1.68	1.63	1.59	1.57
M1ASD25	0.7	1.65	1.59	1.57	1.55
M2ASD75	1.2	1.72	1.66	1.64	1.61
M2ASD50	1.0	1.67	1.64	1.61	1.58
M2ASD25	0.7	1.64	1.58	1.57	1.56
MSIASD75	1.1	1.69	1.64	1.60	1.58
MSIASD50	0.8	1.66	1.62	1.58	1.56
MSIASD25	0.9	1.63	1.58	1.56	1.54

However, the amplitudes of the α-relaxation peaks were decreased for these cured HMM1/ASD samples compared with the cured HMM1 and ASD. This reduction in amplitude was more significant for the M1ASD50 compared with the other samples. Suppression of the molecular motion during glass transition is presumably owing to the increase of the crosslinking density and the existence of the interaction between the organic polymer and inorganic networks for the cured HMM1/ASD samples. The predominant source of the interaction comes from the residual hydroxyl groups on the surface of the SiO_2 network and melamine network [14]. In addition, temperature dependence of the dielectric loss tangent for the cured HMM2 and M2ASD50 is shown in Fig. 8. For cured HMM2, the local motions of β and γ-relaxations were observed in the range of −100°C–50°C. Moreover, the α-relaxation behavior of the cured HMM2 was similar to that of the cured HMM1 and that of the cured M2ASD50 was similar to that of the cured M1ASD50. Each of the two exhibited α-relaxation temperatures almost in the same temperature range, even though the number of reaction sites for HMM2 was less than that for HMM1. This implies that the packing of the rigid aromatic ring through the organic network was able to effectively suppress the molecular motion during glass transition [6,8,31,32]. Moreover, the composition dependence of the dielectric relaxation for the cured HMM2/ASD samples (M2ASD25, M2ASD50, and M2ASD75) are the same as that for the cured HMM1/ASD samples. In addition, dielectric relaxation behavior of the cured HMMSI and HMMSI/ASD samples (MSIASD25, MSIASD50 and MSIASD75) is shown in Fig. 9. The composition dependence of the dielectric relaxation is different from those of the cured HMM1/ASD and HMM2/ASD samples. The α-relaxation temperature increases with the increase in the content of HMMSI because of the high α-relaxation temperature of the cured HMMSI samples. Moreover, the crosslinking between HMMSI and ASD via the sol–gel process results in the suppression of the molecular motion, and subsequently leads to the enhancement of the α-relaxation temperature for the cured HMMSI/ASD samples. This result is more significant for the cured HMMSI/ASD sample containing a higher HMMSI content (above 50 wt.%).

The poling effect on the absorption behavior of the NLO polymer films were measured by UV-Vis spectroscopy. The absorption spectra for the NLO polymer films before and after poling, and under thermal treatments at 100°C are shown in Fig. 10. The maximum of the absorption occurred around 450 nm for these NLO polymers. Immediately after poling/curing, a decrease and a blue shift were observed in the spectrum. This was due to dichroism and electrochromism resulting from the induced dipole alignment [33]. Moreover, the relaxation phenomenon was observed in the spectrum after thermal treatment at 100°C for 250 h. The linear optical properties of these NLO sol–gel materials are summarized in Table 2. The thickness of the polymer films ranged from 0.7 to 1.2 μm. The refraction indices ranged from 1.54 to 1.75, and increased with the increase in the content of ASD. The second-harmonic coefficients d_{33} and d_{31} of poled/cured ASD, HMM1/ASD, HMM2/ASD and HMMSI/ASD samples for incident light of 1064 and 1542 nm are summarized in Table 3. These melamine/ASD based all sol–gel organic–inorganic NLO materials show large second-order nonlinearity after poling and curing at 220°C for 1 h. Moreover, the second-harmonic coefficients increased with the increase in the content of ASD. A larger second-harmonic coefficient of these NLO sol–gel materials was obtained for the incident light of 1064 nm compared with the second-harmonic coefficient obtained at 1542 nm. This is due to the resonant enhancement of the second-harmonic generation at a wavelength near 532 nm [34].

The temporal characteristics of the second harmonic coefficient for the poled/cured NLO sol–gel films at 100°C are shown in Fig. 11. In Fig. 11(a), a better temporal stability was obtained for the poled/cured HMM1/ASD samples compared with the poled/cured ASD, especially the one with an equivalent weight ratio of HMM1 and ASD. The dense and uniform packing of the organic and inorganic networks leads to better temporal stability of the all sol–gel organic–inorganic NLO material. In Fig. 11(b), the composition dependence of the temporal stability for poled/cured HMM2/ASD samples was the same as that for the HMM1/ASD samples. This corroborates that the HMM1/ASD and HMM2/ASD samples show similar thermal dynamic behavior as studied by dielectric spectroscopy. In addition, the temporal stability behavior of the poled/cured HMMSI/ASD samples are shown in Fig. 11(c). Better temporal stability was obtained for the poled/cured HMMSI/ASD sample containing a higher HMMSI content. The temporal stability of the poled/cured ASD could be significantly improved by the incorporation of ASD into the melamine-based sol–gel material.

Table 3
The second harmonic coefficients d_{33} and d_{31} (pm/V) of a series of melamines and an alkoxysilane dye based all sol–gel NLO materials for incident light of 1064 and 1542 nm wavelength

Samples	$d_{33(1064)}$	$d_{31(1064)}$	$d_{33(1542)}$	$d_{31(1542)}$
ASD	54.0	19.2	16.6	6.4
M1ASD75	41.8	13.7	12.0	4.2
M1ASD50	40.0	14.3	11.8	4.8
M1ASD25	17.3	6.2	6.3	2.7
M2ASD75	38.7	14.1	9.3	3.4
M2ASD50	34.3	13.9	9.7	3.9
M2ASD25	16.8	5.4	4.3	1.6
MSIASD75	37.6	12.7	8.8	3.2
MSIASD50	28.1	9.5	8.6	3.1
MSIASD25	10.7	4.6	3.2	1.1

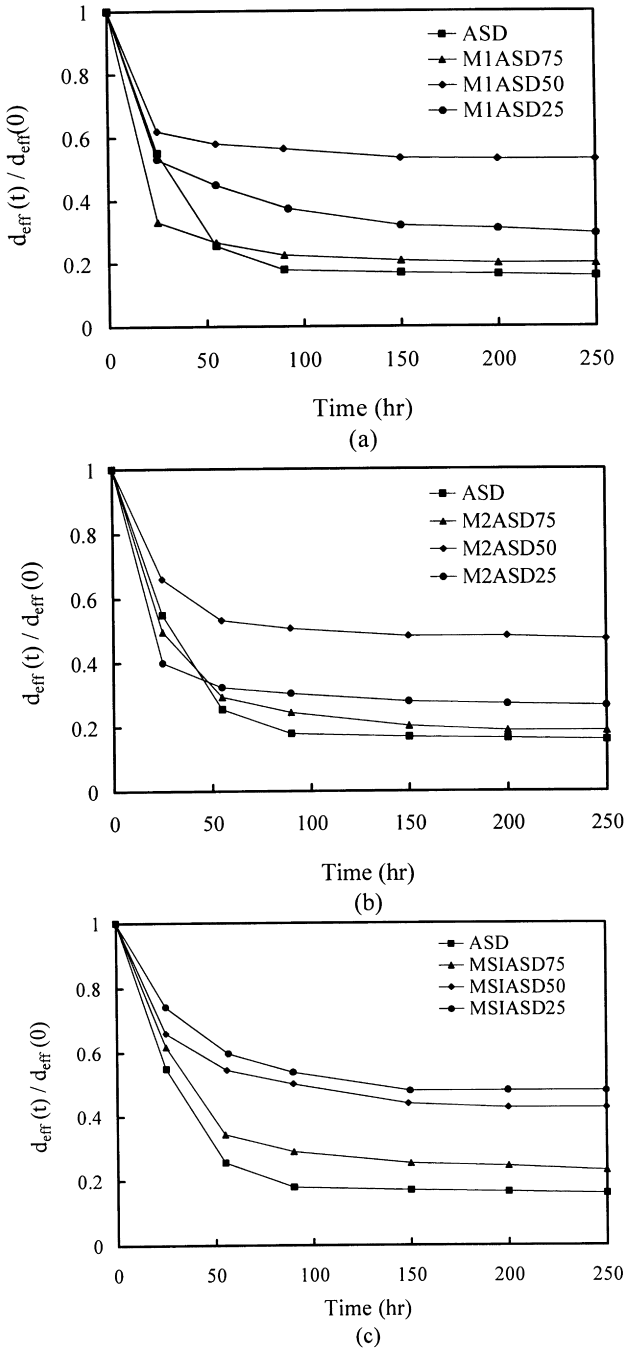

Fig. 11. Temporal behavior of the second-order NLO coefficient for the poled/cured: (a) HMM1/ASD; (b) HMM2/ASD; (c) HMMSI/ASD samples.

4. Conclusion

A series of all sol–gel organic–inorganic materials for second-order nonlinear optics was developed. The cross-linked HMM1/ASD, HMM2/ASD and HMMSI/ASD sol–gel materials are optically clear with no sign of any phase separation as determined by SEM at a magnification of 4000 ×. This series of NLO sol–gel materials exhibits a large second-order optical nonlinearity after poling and curing processes. Dielectric results indicate that the melamines (HMM1, and HMM2) and an ASD based all sol–gel organic–inorganic NLO materials, especially the ones with equivalent weight ratio of melamine and ASD, have a higher glass transition temperature than the cured ASD sample. Moreover, the α-relaxation temperature increases with the increase in the content of HMMSI for the organically modified NLO sol–gel materials. As a result, better temporal stability at 100°C was obtained for these melamine-based sol–gel organic–inorganic materials compared with that for the poled/cured ASD sample.

Acknowledgements

The authors thank the National Science Council of Taiwan, ROC for financial support (Grant NSC87-2216-E007-032). Professor J.T. Shy and Dr T.H. Suen are also thanked for their help and advice on NLO measurements.

References

[1] Prasad PN, Williams DJ. Introduction to nonlinear optical effects in molecules and polymers. New York: Wiley, 1991.
[2] Meredith GR, Dusen JG, Williams DJ. Macromolecules 1982;15:1385.
[3] Wang NP, Leslie TM, Wang S, Kowel ST. Chem Mater 1995;7:185.
[4] Stenger-Smith JD, Henry RA, Hoover JM, Lindsay GA, Nadler MP, Nissan RA. J Polym Sci 1993;31:2899.
[5] Xu C, Wu B, Todorova O, Dalton LR, Shi Y, Ranon PM, Steier WH. Macromolecules 1993;26:5303.
[6] Jeng RJ, Chen YM, Jain A, Tripathy SK, Kuman J. Opt Commun 1992;89:212.
[7] Kim J, Plawsky JL, LaPeruta R, Korenowski GM. Chem Mater 1992;4:249.
[8] Jeng RJ, Chen YM, Chen JI, Kumar J, Tripathy SK. Macromolecules 1993;26:2530.
[9] Wung CJ, Lee KS, Prasad PN, Kim JC, Jin JI, Shim HK. Polymer 1992;33:4145.
[10] Yoshida M, Prasad PN. Chem Mater 1996;8:235.
[11] Lebeau B, Brasselet S, Zyss J, Sanchez C. Chem Mater 1997;9:1012.
[12] Landry CJT, Coltrain BK, Brady BK. Polymer 1992;33:1486.
[13] Noell JLW, Wilkes GL, Mohanty DK, Mcgrath JE. J Appl Polym Sci 1990;40:1177.
[14] Landry CJT, Coltrain BK, Wesson JA, Zumbulyadis N, Lippert JL. Polymer 1992;33:1496.
[15] Brydson JA. Plastics materials. 4. London: Butterworths Scientific, 1982.
[16] Updegraff IH. Encyclopedia of polymer science and engineering. New York: Wiley, 1986.
[17] Jeng RJ, Hsiue GH, Chen JI, Marturunkakul S, Li L, Jiang XL, Moody R, Masse C, Kumar J, Tripathy SK. J Appl Polym Sci 1995;55:209.
[18] Kozakiewicz JJ, Maginess JE. J Appl Polym Sci 1987;34:1109.
[19] Ellsworth MW, Novak BM. J Am Chem Soc 1991;113:2756.
[20] Novak BM, Davies C. Macromolecules 1991;24:5481.
[21] Mandal B, Jeng RJ, Kumar J, Tripathy SK. Makromol Chem, Rapid Commun 1991;12:607.
[22] Mortazavi MA, Knoesen A, Kowel ST, Higgins BG, Dienes AJ. Opt Soc Am 1989;B6:773.
[23] Li L. PhD dissertation. Lowell, MA: University of Massachusetts, 1993.
[24] Jeng RJ, Chen YM, Kumar J, Tripathy SK. J Macromol Sci, Pure Appl Chem 1992;A29:1115.

[25] Mandal BK, Chen YM, Lee JY, Kumar J, Tripathy SK. Appl Phys Lett 1991;58:2459.
[26] Jeng RJ, Chen YM, Jain AK, Kumar J, Tripathy SK. Chem Mater 1992;4:1141.
[27] Premachandra J, Kumudinie C, Zhao W, Mark JEJ. Sol–Gel Sci Tech 1996;7:163.
[28] Stevens G, Richardson M. Polymer 1983;24:851.
[29] Betrabet CS, Wilkes GL. Chem Mater 1995;7:535.
[30] Chen JI, Moody RA, Chen YM, Lee JY, Sengupta SK, Kumar J, Tripathy SK. Mat Res Soc Symp Proc 1992;247:223.
[31] Jeng RJ, Chen YM, Jain AK, Kumar J, Tripathy SK. Chem Mater 1992;4:972.
[32] Tang MY, Mark JE. Macromolecules 1984;17:2616.
[33] Yang Z, Xu C, Wu B, Dalton LR, Kalluri S, Steier WH, Shi Y, Bechtel JH. Chem Mater 1994;6:1899.
[34] Nakayama H, Sugihara O, Okamoto N. Chapter 11. In: Miyata S, Sasabe H, editors. Poled polymers and their applications to SHG and EO devices, Japan: Gordon and Breach Science Publishers, 1997. p. 209.